Proceedings of the ASME 2019 14th International Manufacturing Science and Engineering Conference
MSEC2019
June 10-14, 2019, Erie, PA, USA

MSEC2019-3001

BINDER JETTING ADDITIVE MANUFACTURING OF CERAMICS: FEEDSTOCK POWDER PREPARATION BY SPRAY FREEZE GRANULATION

Wenchao Du
Department of Industrial & Systems Engineering
Texas A&M University
College Station, TX 77843

Guanxiong Miao
Department of Mechanical Engineering
Texas A&M University
College Station, TX 77843

Lianlian Liu
Department of Materials Science & Engineering
Texas A&M University
College Station, TX 77843

Zhijian Pei
Department of Industrial & Systems Engineering
Texas A&M University
College Station, TX 77843

Chao Ma
Department of Engineering Technology & Industrial Distribution
Department of Industrial & Systems Engineering
Department of Mechanical Engineering
Department of Materials Science & Engineering
Texas A&M University
College Station, TX 77843

ABSTRACT

Objective of this study is to prepare the binder jetting feedstock powder by spray freeze drying and study the effects of its parameters on the powder properties. Binder jetting additive manufacturing is a promising technology for fabricating ceramic parts with complex or customized geometries. However, this process is limited by the relatively low density of the fabricated parts even after sintering. The main cause comes from the contradicting requirements of the particle size of the feedstock powder: a large particle size (>5 μm) is required for a high flowability while a small particle size (<1 μm) for a high sinterability. For the first time, a novel technology for the feedstock material preparation, called spray freeze drying, is investigated to address this contradiction. Using raw alumina nanopowder (100 nm), a full factorial design at two levels for two factors (spraying pressure and slurry feed rate) was formed to study their effects on the properties (i.e., granule size, flowability, and sinterability) of the obtained granulated powder. Results show that high pressure and small feed rate lead to small granule size. Compared with the raw powder, the flowability of the granulated powders was significantly increased, and the high sinterability was also maintained. This study proves that spray freeze granulation is a promising technology for the feedstock powder preparation of binder jetting additive manufacturing.

1. INTRODUCTION

Ceramic materials have outstanding properties, such as extraordinary hardness, excellent resistance to wear, heat, and corrosion, and exceptional biocompatibility [1]. However, it is very costly to fabricate ceramic parts of complex shapes using conventional manufacturing techniques. For complex ceramic parts, tooling can contribute to up to 80 % of the overall cost if traditional processing routes are taken [2]. Compared with that, additive manufacturing (AM), also known as 3D printing, has many advantages, including flexible and customized design, elimination of special fabrication tooling, and efficient usage of raw materials. Therefore, AM of ceramic materials have attracted a lot of research interest [3]. Among all AM technologies, binder jetting is considered the most promising for printing ceramic materials because it is easy to scale up and it does not require support [4].

A high density of a ceramic part is usually desirable for the load-bearing applications, such as artificial human joints [5]. However, the achieved density of the printed parts from binder jetting is relatively low even after sintering [1]. Currently, the bulk density [6] of ceramic parts by this process ranges from 40% to 68% [7–12], far below the requirement for load-bearing applications. The main cause comes from the contradicting requirements for the particle size of the feedstock powder: a large particle size (>5 μm) is required for a high flowability while a small particle size (<1 μm) for a high sinterability. Granulation

has been attempted to address this contradiction [1]. By granulating fine particles into coarse granules, the granulated powder will maintain the high sinterability of the fine particles and increase the flowability by the increased size. Among many different granulation methods reported in the literature, spraying drying (SD) is the most common one [13–19]. However, some of its disadvantages impeded its application. For example, spray-dried granules usually show a hollow structure due to the rapid mass transport of the binder liquid from the center to the shell of the granule during the evaporation drying, which leads to inhomogeneous microstructures of the part [20]. The hard shell of SD granules will make them difficult to break and thus result in inter-granule porosity [20,21].

Another granulation method, called spray freeze drying (SFD), has attracted interest for the ceramic material preparation [20–25]. As this technology uses a drying route of freezing-sublimation, the mass transport is slow and controlled during the drying step, which makes the microstructure of the granules homogeneous. For example, Raghupathy *et al*. [20] prepared granulated zirconia powder by both spraying drying and spray freeze drying. Although both powders achieved similar flow rates, crushable granules with a low granule strength were obtained only from spray freeze drying, which is beneficial to the microstructure homogeneity of dry-pressed and sintered parts. Ghanizadeh *et al*. [23] prepared granulated alumina powder and characterized its flow rate. Green and sintered densities (densities of the part after curing and sintering, respectively) were measured for dry-pressed disk samples to investigate the effect of the sintering profile on the grain growth.

Despite some existing studies on spray freeze drying of ceramic materials, the effects of the spraying pressure and slurry feed rate on the flowability and sinterability of the granulated powder has not been studied. This study aims at filling this knowledge gap by carrying out experiments based on a full factorial design. The granule size and morphology were characterized, and the flow rate of the obtained powder and the density of dry-pressed and sintered disk samples were studied. Finally, discussion was created based on the results.

2. EXPERIMENTAL METHODS

2.1 Slurry preparation

Nano-sized alumina slurry (100 nm, 20 wt. %, Department of Specialty Grains & Powders, Saint-Gobain Ceramic Materials, MA, USA) was used to ensure a high sinterability of the feedstock material. The slurry was frozen in a freezer and then dried in a freeze drier (FreeZone 2.5 L, Labconco, MO, USA) under 1.5 mbar for 12 h to obtain the dry powder. The dried alumina was mixed with deionized water using a ball mill (Laboratory Jar Rolling Mill, Paul O. Abbe, IL, USA) to prepare 20 vol. % slurry for spraying. The ball milling parameters are shown in Table 1.

2.2 Granulated powder preparation

Spray freeze drying includes spray freezing and freeze drying. Figure 1 shows the machine set up (LS-2, PowderPro AB, Sweden) for the spray freezing. A peristaltic pump feeds the slurry into an atomizing nozzle that is above the liquid surface and connected with compressed air. The slurry is atomized into droplets, which are sprayed into liquid nitrogen in the spraying container. The frozen granules are then put on a tray in the drying chamber of the freeze drier to sublimate the water in the granules.

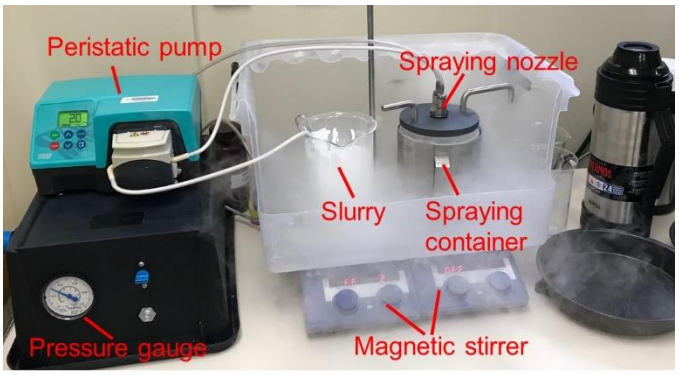

Figure 1. PowderPro LS-2 freeze granulator

To investigate the effects of the granulation parameters (spraying pressure and feed rate), two levels of each parameter were tested to form a full factorial design, as shown in Table 1. Therefore, there were four trials with different combinations of the spraying pressure and feed rate. The freeze drying parameters, as listed in Table 1, were kept fixed across all trials.

Table 1. The parameters for the slurry preparation, spray freezing, and freeze drying

Slurry preparation	Alumina concentration (vol. %)	20
	Ball-to-slurry mass ratio	1:1
	Milling time (h)	12
Spray freezing	Pressure (bar)	0.1 and 0.4
	Feed rate (L/h)	0.5 and 1
Freeze drying	Drying chamber pressure (mbar)	1.5
	Tray temperature (°C)	20
	Collector temperature (°C)	-50
	Drying time (h)	12

2.3 Material characterization

To prepare the sample for the morphology of the raw particles, the diluted slurry was dripped onto the surface of a silicon wafer and was left at the room temperature to be slowly dried. The morphology of the raw particles was characterized by scanning electron microscopy (SEM, JSM-7500F, JEOL, Japan). After granulation, the morphology of the obtained granules was characterized by another SEM (TESCAN VEGA II LSU, Brno-Kohoutovice, Czech Republic). The granule size was studied by sieve analysis. An eight-inch sieve set with opening sizes of 25, 53, 75, 90, and 250 μm was used.

As a feedstock powder with a particle size smaller than 25 μm or larger than 250 μm is rarely used in binder jetting, granulated powders within size ranges of 25–53, 53–75, 75–90, and 90–250 μm from all four trials were used for the measurement of flowability and sinterability. Flowabilities of the raw and granulated (25–250 μm) powders were tested by measuring the flow rate, i.e., the weight of falling granules

through a funnel with an opening of Φ2.54 mm (DF-1-02, Hongtuo Instrument, China) in one second.

For the sinterability test, these powders were dry-pressed at 100 MPa into disks of Φ12.7 mm by a hydraulic cold press (Carver Laboratory Press, Model C, Fred S. Carver Inc., IN, USA). The pressed disks were then sintered at 1600 °C for 2 h and cooled to the room temperature in a bench-top muffle furnace (KSL-1700X-A1-UL, MTI Corp., CA, USA). A disk sample from the raw powder was prepared as well for comparison. Sinterabilities of the raw and granulated powders were tested by measuring the relative sintered density of the disk samples using a density kit (Torbal AGCN200, Scientific Industries Inc., NJ, USA). The sintered density was measured based on the ISO standard [6]. Specifically, dry mass (m_1) was measured after sintering and cooling. Then the sample was boiled in deionized water for 2 h and then cooled to the room temperature. The mass of the sample in water (m_2) was measured by the density kit and then the sample was wiped by a wet cloth to remove the water on the surface, followed by the measurement of the mass of the wiped sample (m_3). The relative sintered bulk density (ρ) of the sample was calculated based on the following equation:

$$\rho = \frac{\rho_{wt}}{\rho_{th}} \times \frac{m_1}{m_3 - m_2} \times 100\% \qquad (1)$$

where ρ_{wt} is the water density at the temperature when taking the measurement and ρ_{th} is the theoretical density of the alpha-phase alumina (3.97 g/cm^3).

3. RESULTS AND DISCUSSION

Figure 2 shows the SEM of the raw powder in the spraying slurry. The particle has an irregular shape and its size is around 100 nm.

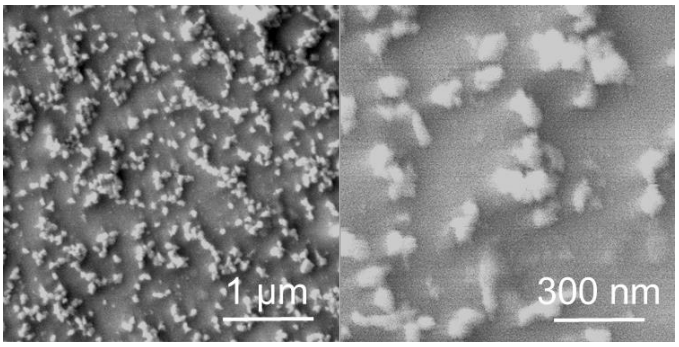

Figure 2. SEM of the raw 100 nm powder

The SEM of the granulated powders from different trials are shown in Figure 3. The shape of the granules is spherical. Granules from Trials 2–4 evidently present a satellite structure, i.e., small granules firmly attach to a larger one. Based on a comparison between Trial 1 and Trial 3, higher spraying pressure leads to a greater extent of satellite structures. Similarly, a comparison between Trial 2 and Trial 4 leads to the same result. Based on a comparison between Trial 3 and Trial 4, higher feed rate leads to a greater extent of satellite structures. Similarly, a comparison between Trial 1 and Trial 2 leads to the same result. In summary, the spraying pressure and feed rate significantly affect the extent of satellite structure. Higher spraying pressure and higher feed rate lead to a greater extent of satellite structure, resulting in the greatest extent of satellite structure for the powder from Trial 4. One of the reasons is that higher spraying pressure creates more fine droplets, and higher feed rate increases the amount of the sprayed droplets in a unit time, both of which lead more collisions between the sprayed droplets in the spraying container and consequently a great extent of satellite structure in the granulated powder.

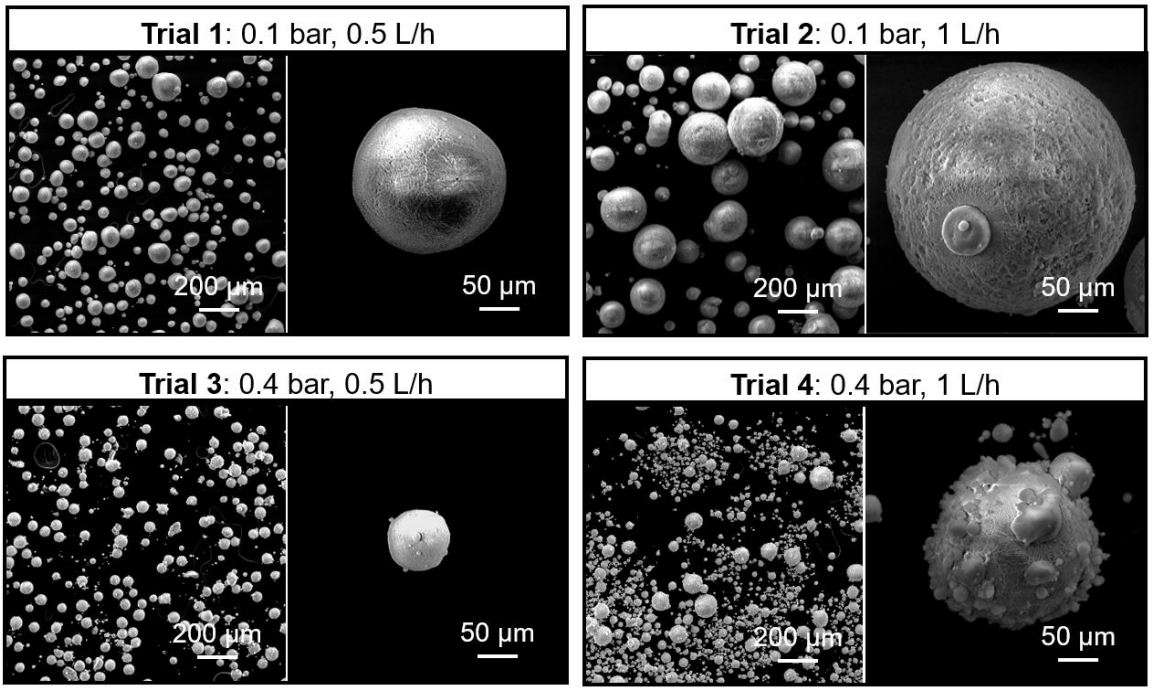

Figure 3. SEM of granules from all four trials

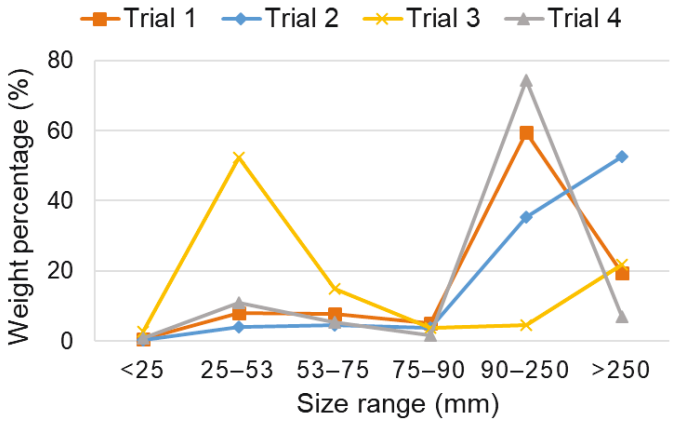

Figure 4. Weight percentages of different size ranges of the granulated powder from different experiments

Figure 4 shows the results of the sieve analysis of all four trials. The dominant size ranges are 90–250, >250, 25–53, and 90–250 μm for Trials 1–4, respectively. The seive analysis result agrees well with the SEM charaterization. Based on the sieve analysis result in Figure 4, it can be concluded that higher spraying pressure leads to smaller granule size at the same feed rate. At the same feed rate of 0.5 L/h, for example, the increase of the spraying pressure (Trial 1 to Trial 3) led to a decrease of the dominant size range from 90–250 μm to 25–53 μm. On the other hand, higher feed rate leads to larger granule size at the same spraying pressure. At the same spraying pressure of 0.4 bar, for example, the increase of the feed rate (Trial 3 to Trial 4) led to an increase of the dominant granule size range from 25–53 to 90–250 μm. In summary, the spraying pressure and feed rate significantly affect the granule size. Higher spraying pressure and lower feed rate lead to smaller granule size, resulting in the smallest dominant size range of 25–53 μm for the granulated powder from Trial 3.

Table 2 shows the flow rates of the raw and granulated powders and the sintered densities of the disk samples from these powders. In some cases, the powder has a too low flowability to fall through the funnel opening and no value was obtained for the flow rate test. To explain the flow rate results, it is needed to examine the forces that are applied on the granules. Among all the forces, gravity is dominant for large granules while interparticle forces, such as van der Waals and electrostatic forces, are dominant for small granules. Therefore, large granules tend to flow easily while small ones not due to interparticle friction and agglomeration [26]. As shown in Table 2, it can be concluded that granule size significantly affects its flowability. For the granulated powder within the same trial, the flowability increases (or stay the same) as the size increases. Another factor that affects the flowability of the granulated powder is the extent of the satellite structure, which will decrease the flowability due to the increased inter-granule friction. As shown in Figure 3, the granulated powder from Trial 1 has the least extent of satellite structure. Within the same size range, the flow rate of the granulated powder from Trial 1 is larger than (or equal to) that of granulated powders from all other trials. On the other hand, granulated powder from Trial 4 has the greatest extent of satellite structure. Within the same size range, the flow rate of the granulated powder from Trial 4 is less than (or equal to) that of granulated powders from all other trials.

Table 2. Flowability and sinterability test results of raw and granulated powders

Trial	Size (μm)	Flow rate (g/s)	Relative sintered density (%)
Raw	0.1	/	93.4
1	25–53	0.06	96.7
	53–75	0.19	95.0
	75–90	0.24	98.0
	90–250	0.24	96.2
2	25–53	/	97.0
	53–75	0.19	94.6
	75–90	0.20	96.1
	90–250	0.24	91.6
3	25–53	/	93.5
	53–75	0.09	97.2
	75–90	0.10	94.6
	90–250	0.21	96.2
4	25–53	/	96.2
	53–75	0.08	95.7
	75–90	0.10	94.9
	90–250	0.10	96.9

Sinterability is another important factor of the feedstock material for the binder jetting process. Under the same conditions, a material with high sinterability leads to high sintered density of the printed part [1], and a sintered density of larger than 90% usually indicates a good sinterability. After granulation, the high sinterability of the raw alumina powder was maintained (or even increased in most cases) in the spray-freeze-dried granulated powders. Reasons for the increase of the sintered density include the flowability improvement after granulation and subsequently more dense packing of the granules of the disk sample after pressing.

4. CONCLUSIONS

Experimental trials based on a full factorial design of spraying pressure and slurry feed rate were carried out to study their effects on the granule size, flowability, and sinterability of the granulated powder. Size analysis results show that high spraying pressure and low feed rate lead to small granule size. Morphology analysis revealed the satellite structure in the granulated powder, whose extent increased as the spraying pressure and feed rate increased. Larger granule size and less extent of satellite structure led to higher flow rate and better flowability. Moreover, sintered densities of the disk samples from most of the granulated powders are higher than that of the raw powder. This study could guide the feedstock powder preparation process for ceramic binder jetting additive manufacturing by spraying freeze drying.

ACKNOWLEDGEMENTS

This material is based upon work supported by the National Science Foundation under Grant No. 1762341. The authors acknowledge Mr. Jim Salvatore and Dr. Stephen Bottiglieri from Saint-Gobain for their support of the raw material. The authors also thank Mr. Martin Sjöstedt from PowderPro AB for his helpful advice about the slurry preparation.

REFERENCES

[1] Du, W., Ren, X., Ma, C., and Pei, Z., 2017, "Binder Jetting Additive Manufacturing of Ceramics: A Literature Review," *Proceedings of the ASME 2017 International Mechanical Engineering Congress and Exposition*, Tampa, FL, pp. 1–12.

[2] Klocke, F., 1997, "Modern Approaches for the Production of Ceramic Components," J. Eur. Ceram. Soc., 17(2–3), pp. 457–465.

[3] Deckers, J., Vleugels, J., and Kruth, J. P., 2014, "Additive Manufacturing of Ceramics: A Review," J. Ceram. Sci. Technol., 5(4), pp. 245–260.

[4] Du, W., Ren, X., Ma, C., and Pei, Z., 2019, "Ceramic Binder Jetting Additive Manufacturing: Particle Coating for Increasing Powder Sinterability and Part Strength," Mater. Lett., 234, pp. 327–330.

[5] Du, W., Ren, X., Chen, Y., Ma, C., Radovic, M., and Pei, Z., 2018, "Model Guided Mixing of Ceramic Powders with Graded Particle Sizes in Binder Jetting Additive Manufacturing," *Proceedings of the ASME 2018 13th International Manufacturing Science and Engineering Conference*, College Station, TX, pp. 1–9.

[6] ISO, 2013, "ISO 18754:2013 Fine Ceramics (Advanced Ceramics, Advanced Technical Ceramics) – Determination of Density and Apparent Porosity."

[7] Mehrban, N., Bowen, J., Vorndran, E., Gbureck, U., and Grover, L. M., 2013, "Structural Changes to Resorbable Calcium Phosphate Bioceramic Aged in Vitro," Colloids Surfaces B Biointerfaces, 111, pp. 469–478.

[8] Sheydaeian, E., Vlasea, M., Woo, A., Pilliar, R., Hu, E., and Toyserkani, E., 2016, "Effect of Glycerol Concentrations on the Mechanical Properties of Additive Manufactured Porous Calcium Polyphosphate Structures for Bone Substitute Applications," J. Biomed. Mater. Res. - Part B Appl. Biomater., 105(4), pp. 828–835.

[9] Dcosta, D. J., Sun, W., Lin, F., and Ei-Raghy, T., 2002, "Freeform Fabrication of Ti3SiC2 Powder-Based Structures: Part II - Characterization and Microstructure Evaluation," J. Mater. Process. Technol., 127(3), pp. 352–360.

[10] Shanjani, Y., Amritha De Croos, J. N., Pilliar, R. M., Kandel, R. A., and Toyserkani, E., 2010, "Solid Freeform Fabrication and Characterization of Porous Calcium Polyphosphate Structures for Tissue Engineering Purposes," J. Biomed. Mater. Res. - Part B Appl. Biomater., 93(2), pp. 510–519.

[11] Tarafder, S., Balla, V. K., Davies, N. M., Bandyopadhyay, A., and Bose, S., 2013, "Microwave-sintered 3D Printed Tricalcium Phosphate Scaffolds for Bone Tissue Engineering," J. Tissue Eng. Regen. Med., 7(8), pp. 631–641.

[12] Suwanprateeb, J., Sanngam, R., and Suwanpreuk, W., 2008, "Fabrication of Bioactive Hydroxyapatite/Bis-GMA Based Composite via Three Dimensional Printing," J. Mater. Sci. Mater. Med., 19(7), pp. 2637–2645.

[13] Warnke, P. H., Seitz, H., Warnke, F., Becker, S. T., Sivananthan, S., Sherry, E., Liu, Q., Wiltfang, J., and Douglas, T., 2010, "Ceramic Scaffolds Produced by Computer-assisted 3D Printing and Sintering: Characterization and Biocompatibility Investigations," J. Biomed. Mater. Res. - Part B Appl. Biomater., 93(1), pp. 212–217.

[14] Becker, S. T., Bolte, H., Krapf, O., Seitz, H., Douglas, T., Sivananthan, S., Wiltfang, J., Sherry, E., and Warnke, P. H., 2009, "Endocultivation: 3D Printed Customized Porous Scaffolds for Heterotopic Bone Induction," Oral Oncol., 45(11), pp. e181–e188.

[15] Castilho, M., Moseke, C., Ewald, A., Gbureck, U., Groll, J., Pires, I., Teßmar, J., and Vorndran, E., 2014, "Direct 3D Powder Printing of Biphasic Calcium Phosphate Scaffolds for Substitution of Complex Bone Defects," Biofabrication, 6(1), p. 015006.

[16] Fierz, F. C., Beckmann, F., Huser, M., Irsen, S. H., Leukers, B., Witte, F., Degistirici, Ö., Andronache, A., Thie, M., and Müller, B., 2008, "The Morphology of Anisotropic 3D-Printed Hydroxyapatite Scaffolds," Biomaterials, 29(28), pp. 3799–3806.

[17] Seitz, H., Deisinger, U., Leukers, B., Detsch, R., and Ziegler, G., 2009, "Different Calcium Phosphate Granules for 3-D Printing of Bone Tissue Engineering Scaffolds," Adv. Eng. Mater., 11(5), pp. 41–46.

[18] Seidenstuecker, M., Kerr, L., Bernstein, A., Mayr, H., Suedkamp, N., Gadow, R., Krieg, P., Hernandez Latorre, S., Thomann, R., Syrowatka, F., and Esslinger, S., 2017, "3D Powder Printed Bioglass and β-tricalcium Phosphate Bone Scaffolds," Materials (Basel)., 11(1), p. 13.

[19] Suwanprateeb, J., Sanngam, R., and Panyathanmaporn, T., 2010, "Influence of Raw Powder Preparation Routes on Properties of Hydroxyapatite Fabricated by 3D Printing Technique," Mater. Sci. Eng. C, 30(4), pp. 610–617.

[20] Raghupathy, B. P. C., and Binner, J. G. P., 2011, "Spray Granulation of Nanometric Zirconia Particles," J. Am. Ceram. Soc., 94(1), pp. 42–48.

[21] Moritz, T., and Nagy, A., 2002, "Preparation of Super Soft Granules from Nanosized Ceramic Powders by Spray Freezing," J. Nanoparticle Res., 4(5), pp. 439–448.

[22] Binner, J., and Vaidhyanathan, B., 2008, "Processing of Bulk Nanostructured Ceramics," J. Eur. Ceram. Soc., 28(7), pp. 1329–1339.

[23] Ghanizadeh, S., Ramanujam, P., Vaidhyanathan, B., and Binner, J., 2016, "Spray Freeze Granulation of Submicrometre α-alumina Using Ultrasonication," J. Ceram. Sci. Technol., 7(4), pp. 455–461.

[24] Zhang, Y., Binner, J., Rielly, C., and Vaidhyanathan, B., 2014, "Comparison of Spray Freeze Dried Nanozirconia Granules Using Ultrasonication and Twin-fluid Atomisation," J. Eur. Ceram. Soc., 34(4), pp. 1001–1008.

[25] Liu, W., and Zhipeng, X., 2015, "Spray Freeze Granulation of Submicron Alumina and Its Sintering Behavior via Spark Plasma Sintering," Sci. Sinter., 47(3), pp. 279–288.

[26] Yang, J., Sliva, A., Banerjee, A., Dave, R. N., and Pfeffer, R., 2005, "Dry Particle Coating for Improving the Flowability of Cohesive Powders," Powder Technol., 158(1–3), pp. 21–33.